Evidence for the Delayed Oscillator Mechanism for ENSO: The "Observed" Oceanic Kelvin Mode in the Far Western Pacific*

NATHAN J. MANTUA AND DAVID S. BATTISTI

Department of Atmospheric Sciences, University of Washington, Seattle, Washington

1 April 1993 and 11 August 1993

ABSTRACT

Observed surface winds from 1961 through September 1992 are used to force a reduced gravity shallow water ocean model. Results from the hindcast of ocean variability are found to be consistent with the results Li and Clarke presented in a previous study of sea level and zonal wind variability in the tropical Pacific. In this note the apparent discrepancies are reconciled between "delayed oscillator" theory and calculated lag correlations between the observationally based records of western boundary Kelvin mode amplitude (η_w) and zonal wind forcing. Evidence for sensitivity in these "delayed oscillator" lag correlations is presented from a variety of sources, including: the hindcast data, output from the standard version of the Zebiak and Cane coupled ocean–atmosphere model, and through three cases with idealized time series of ENSO variability. The authors demonstrate that the low lag correlations for η_w leading the zonal wind forcing by 1 to 1½ years is not *inconsistent* with the hypothesized role of western boundary reflections as the ultimate termination mechanism for ENSO anomalies. The lack of regularity in the system studied guarantees a degraded correlation for η_w leading the zonal wind by 1 to 1½ years. This lack of regularity is not contained in, nor explained by, delayed oscillator theory.

A robust feature in all of the records examined in this work is the existence of upwelling Kelvin signals in the far western equatorial Pacific Ocean due to the developing warm (ENSO) events. The amplitude of the observed Kelvin signals in the western Pacific is sufficient to terminate the developing ENSO events via the delayed oscillator mechanism.

1. Introduction

The "delayed oscillator" paradigm for ENSO stems from theoretical studies and studies using numerical models of the coupled tropical atmosphere and Pacific Ocean system. Many of the theoretical and numerical modeling studies have found that the important interactions between the atmosphere and ocean for the *evolution* of ENSO are in the central and eastern Pacific because the basic state of the tropical upper ocean and the troposphere is strongly nonuniform (particularly in the east to west asymmetry in the ocean thermocline).

Many of these numerical studies employ numerical models of intermediate level complexity where upper-ocean models are coupled to two-layer models of the troposphere (e.g., Zebiak and Cane 1987, hereafter ZC; Schopf and Suarez 1988, hereafter SS88). In these models, the anomalous forcing of the atmosphere is initiated by sea surface temperature (SST) anomalies. In both the observations and in these intermediate models, SST anomalies are extremely small in the western Pacific. Furthermore, in the models there is very little wind anomaly in the western Pacific. Thus, the feedback between the atmosphere and ocean is essentially limited to the central and eastern Pacific. As a result, the interannual variability in the models is quasi stationary, and the ocean signals are transmitted from the interactive (ocean forcing) region to and throughout the western part of the basin without inducing SST anomalies (i.e., they travel freely).

The quasi stationary nature of the simulated (and observed) ENSO events, and the analysis of the physics and thermodynamics of these ENSO events, led SS88 and Battisti (1988) to greatly simplify the physics to two important processes acting on comparable time scales: the ocean basin adjustment time and the strength of the local atmosphere–ocean feedback in the central and eastern Pacific [both processes are fast, O(6–8 months), compared to the ENSO cycle]. The ocean basin adjustment is accomplished by eastward propagating Kelvin signals and westward propagating Rossby modes (mainly, the gravest mode).

The subsequent delayed oscillator paradigm for the model ENSO physics was first postulated by Schopf (1987) (see also Suarez and Schopf 1989, hereafter

* Contribution Number 226 to the Joint Institute for the Study of the Atmosphere and Oceans.

Corresponding author address: Dr. David S. Battisti, Department of Atmospheric Sciences, (AK-40), University of Washington, Seattle, WA 98195.

© 1994 American Meteorological Society

Unauthenticated | Downloaded 12/05/23 06:20 PM UTC

SS89) and then derived by Battisti and Hirst (1989, hereafter BH) from a numerical model very similar to the ZC coupled model. In this theory of ENSO, a growing warm event in the central and eastern tropical Pacific generates Rossby signals in the ocean that propagate freely westward, reflect off the Indonesian landmass, and return to the forcing region as upwelling Kelvin signals. A warm event lasts for about one year and is terminated by the upwelling Kelvin signals that are generated by the warm event itself. The ensuing cold event is thus assured because of the residual Rossby signal in the western basin due to the warm event. The peak amplitude of the cold event is about six months after the peak of the warm event (or about 18 months after the warm event onset), and is characterized by negative zonal wind stress anomalies in the central Pacific.

Thus, "delayed oscillator physics" is a physics that explains the shutdown of a warm (ENSO) event *and* the subsequent generation of the cold event. We stress that in this scenario the initial forcing, or cause for the perturbation responsible for the onset of the warm event is incidental to the delayed oscillator physics; the latter describes the physics of the evolving warm event, the event demise, and the ensuing cold event. In the numerical models of the coupled atmosphere–ocean system, the reflected Kelvin signals are fundamental to the warm event termination and ensure a cold event will immediately follow a warm event [consistent with Rasmusson and Carpenter's (1982) composite canonical ENSO event].

In a companion note, Li and Clarke (1994, hereafter LC) examined the relationship between an index of the observed zonal wind stress anomalies in the equatorial Pacific, τ^b (defined in section 2c), and the "observed" amplitude of the equatorial Kelvin wave in the western Pacific (η_w) expressed as the sea level perturbation on the equator that is due to the equatorial Kelvin wave. On the interannual time scale, ENSO accounts for a substantial portion of the variance in the tropical Pacific atmosphere–ocean system. The delayed oscillator theory of ENSO requires that the Kelvin amplitude in the western Pacific be intimately tied to the central and eastern Pacific zonal wind stress anomaly. Specifically, the existence of upwelling (negative) Kelvin signals in the western Pacific (about 3 months after the onset of ENSO) must precede both the warm event demise by approximately 9 months and the peak of the ensuing cold event, 6 months later. Hence, upwelling Kelvin signals should precede the negative zonal wind stress anomaly of the cold event by approximately 15 months. The lag–lead relationship between the zonal wind stress index and η_w from the Battisti version of the ZC model is displayed in Fig. 1b. The correlation between η_w and τ^b at 14 to 16 months is the focus of LC's note and of our note.

The correlation between η_w and τ^b at 12–16 months, which we will call the *delayed oscillator correlation* for convenience, is nearly unity in the Battisti model. This high correlation exists in the model for two reasons: the model interannual variability is cyclic *and,* equally important, the period of oscillation is nearly constant throughout the entire simulation. Any interruptions or changes in the frequency of the warm-to-cold-to-warm cycles will degrade the delayed oscillator correlation. In Battisti's model this correlation is less than unity due to small changes in the period of the simulated ENSO variability from one warm–cold couplet to the next.

Li and Clarke have calculated the lag-lead correlations between the observed τ^b and a measure of η_w based on Darwin tide gauge data and sound theory of equatorial wave propagation in the presence of islands for the years 1963–85. Their result is also displayed in Fig. 1b. There is no significant positive correlation near 14 months. Li and Clarke conclude that the "delayed oscillator physics" for ENSO is not consistent with the tide gauge data and the observed wind stress.

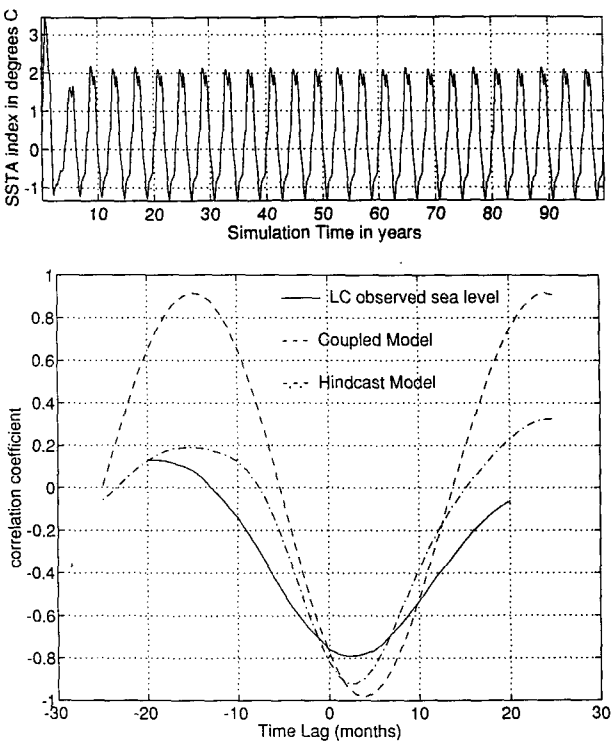

FIG. 1. (a) Time series of NINO3 SST anomalies from a 100-year integration of the standard Battisti version of Zebiak and Cane's coupled model. (b) Lag correlations between the observed zonal wind stress anomalies in the equatorial Pacific and a measure of the Kelvin mode amplitude, η_w, in the far western Pacific (from Clarke 1991; see text). Solid line depicts correlations using the observed η_w and the observed τ^b, 1963–1985; dashed-dot line shows correlations calculated from the coupled model output (from Fig. 1a); dashed line shows correlations using the 1-year low-pass filtered hindcast η_w and the observed τ^b (see section 2). Negative lags indicate η_w leading the zonal wind index.

Unauthenticated | Downloaded 12/05/23 06:20 PM UTC

Wakata and Sarachik (1991, hereafter WS) also examined the equatorial wave activity during the ENSO events. In their study a linearized equatorial β-plane model of the tropical Pacific Ocean was forced by the observed winds for the period 1961–1988. They used the same wind stress data as did LC and concluded, on the basis of Kelvin amplitudes relative to warm and cold events, that the ocean model response to the observed wind stress forcing *is* consistent with the delayed oscillator physics scenario of ENSO: the opposite conclusion reached by LC.

In this paper we will focus on the discrepancy between the delayed oscillator correlation from the observations and that from the quasi-periodic model (Fig. 1). We will argue that because ENSO events are not purely harmonic in nature, the delayed oscillator physics for the ENSO event evolution does not require a large delayed oscillator correlation coefficient between η_w and τ^b. Furthermore, we demonstrate that the record of the observed Kelvin wave amplitude in the western Pacific of LC is in fact *consistent* with the delayed oscillator physics mechanism for the termination of the ENSO events.

2. A hindcast of ocean variability in the tropical Pacific

a. Motivation

In this section we discuss the results of a hindcast experiment that uses observed monthly wind stress anomaly fields as the forcing for the reduced gravity ocean model. This work repeats a calculation done by many others (including Busalacchi and O'Brien 1981; Busalacchi et al. 1983; White et al. 1985; White et al. 1989; Kubota and O'Brien 1988; Zebiak 1989; and WS) with a slightly longer wind record. The previous studies looked at the variability of the ocean model's active upper layer. The purpose of our hindcast experiment is to examine the relationship between the observed zonal wind stress anomalies and both the hindcast and observed record of the western boundary Kelvin mode amplitude (η_w).

b. Model and hindcast procedure

An ocean model was forced with the observed surface wind stress anomalies from The Florida State University analysis (Legler and O'Brien 1988) beginning with January 1961 and ending with September 1992. The ocean model we use for this hindcast study is a replica of the ocean component of the Zebiak and Cane coupled model (built by Battisti 1988) and was used to produce the coupled model results shown in Fig. 1b. The dynamical component of the model is a 1½-layer shallow water model of the tropical Pacific, with parametized surface layer thermodynamics (for details see ZC 1987 or Battisti 1988). The hindcast anomalies were calculated as the departures from the climatological monthly means based on the first 31 years of the data (1961–1991). Dimensional stresses were calculated by multiplying the pseudostress anomalies by the normalization factor $\rho_a C_D = 1.8 \times 10^{-3}$ kg m^{-3} (see also section 5).

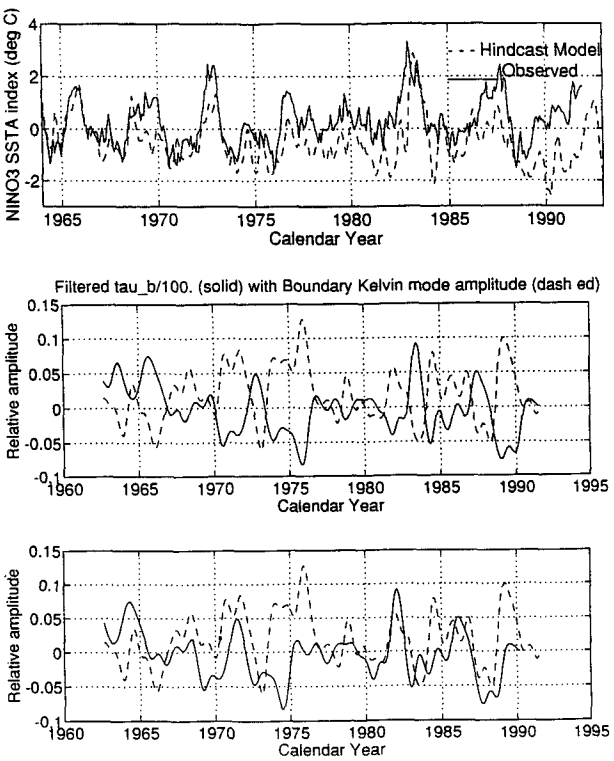

FIG. 2. (a) Time series of the observed (solid) and hindcast (dashed) NINO3 SST anomalies for the period of 1964 through September 1992. (b) Time series of the observed wind stress anomaly τ^b (dashed) and hindcast Kelvin mode amplitude η_w (solid line). The units are nondimensionalized. (c) As in (b) but with $\eta_{w(t+16\text{ months})}$ and $\tau^b(t)$.

The first 4 years of integration are not included in the subsequent analysis to avoid any spinup problems. Time series of the modeled and observed SST anomalies in the NINO3 region (5°N–5°S, 150°W–90°W) are shown in Fig. 2a. The time series for the hindcast Kelvin wave amplitude and the basinwide average of the zonal wind stress anomaly, τ^b, in the equatorial Pacific are displayed in Figs. 2b and 2c.

c. Results: The delayed oscillator lag correlations

Lag correlations were calculated between the hindcast η_w and two indices of the equatorial zonal wind stress anomalies: the first, τ^c, is for the central equatorial Pacific region (4°N–4°S, 160°E–164°W); and the second is the basinwide zonal wind stress index τ^b (4°N–4°S, 124°E–80°W).[1] A 1-year low-pass filter was

[1] In this study we use τ^b as the wind index of interest to better

Unauthenticated | Downloaded 12/05/23 06:20 PM UTC

applied to each time series. Figure 1b shows the lag correlations between η_w and the wind indices for years 1964 through 1991 of the ocean model output. Overall, the correlations between η_w and τ^b from the hindcast data agree well with that calculated by LC (Fig. 1b, or LC's Fig. 5) using the same wind stress indices and a record of η_w calculated from sea level data. The hindcast η_w has a peak correlation with both zonal wind indices when it lags them by two or three months (with τ^b, $r = -0.92$; with τ^c, $r = -0.90$; both correlations exceed the 99% confidence threshold for significance); LC also found a peak correlation when their reconstructed η_w lags the zonal winds by two or three months (with $r \sim -0.8$). This strong negative correlation is predicted by linear equatorial adjustment theory: an equatorially confined wind forcing (e.g., a westerly stress) generates Rossby mode signals (negative or upwelling) to the west of the forcing region. These westward propagating signals eventually strike the western boundary a few months later. In the long-wave, low-frequency limit the zonal mass flux these disturbances carry is returned to the basin interior in the form of eastward propagating Kelvin modes (Cane and Sarachik 1979). The delay time of 2–4 months compares well with the theoretically predicted value.

The delayed oscillator correlation, where η_w *leads* the zonal wind indices by ~14–15 months, has a peak correlation near $r = +0.20$ for both τ^c and τ^b in the hindcast (Fig. 1b and Table 1). The hindcast correlations are statistically indistinguishable from those calculated from the reconstructed η_w and the same zonal wind indices (LC). Without question, the hindcast and observed ocean data do not display the strong positive correlations between η_w and the zonal wind indices that are expected from harmonic, delayed oscillator theory (BH 1989, SS89) and are evident in the coupled model (Fig. 1b) from which the theory was derived.

capture the significant wind anomalies that are east of 164°W. As noted by LC, however, the qualitative features displayed in the lag–lead correlations (summarized in Table 1) are not sensitive to the choice of the wind index, τ^b or τ^c.

3. ENSO regularity and the "delayed oscillator" lag correlations

The Zebiak and Cane (1987) coupled model provides another source for looking at delayed oscillator correlations in a system that displays variability more like that of the observed ENSO. Specifically, their model does not always produce regular and robust interannual variability. Shown in Fig. 3a is the time series of the NINO3 SST anomaly from a 100-year integration of the standard ZC model. Evident in this record is the existence of two relatively distinct regimes: in years 1–50 interannual variability is weak and infrequent, while in years 50–100 the coupled system shows nearly regular and much stronger oscillations between warm and cold phases of the simulated ENSO. The characteristics and physics of the interannual variability in the ZC model in simulation years 50–100 are similar to those in Battisti's version of the ZC model, displayed in Fig. 1 (see also Battisti 1988).

We have split the output from the ZC model at year 50 and will refer to the first 50 years as the "quiescent ENSO" regime, and the last 50 years as the "active ENSO" regime. The lag correlations between η_w and τ^b for the two regimes are shown in Fig. 3b. In the active regime the peak delayed oscillator correlation far exceeds that calculated from the quiescent regime. For η_w leading τ^b, the correlation peaks at $r = +0.71$ in the active regime compared with $r = +0.33$ in the quiescent regime (these correlations differ significantly

TABLE 1. Summary of the peak delayed-oscillator lag correlations: r_{max} is the peak delayed oscillator lag correlation between the variables listed in the table heading; *dt* is the lag time (in months) by which η_w leads the zonal wind index for the correlation coefficient listed. Confidence intervals (*ci*) for an assumed independent sampling interval of 1 year are also listed when greater than 90%.

	η_w leads τ^c			η_w leads τ^b		
Source	r_{max}	*ci* (%)	*dt* (months)	r_{max}	*ci* (%)	*dt* (months)
Li and Clarke						
reconstructed η_w from tide gauge records and FSU wind data, 1963–1985	0.10	—	18	0.10	—	18
Hindcast η_w						
1964–1991	0.22	—	14	0.19	—	14
1964–1976	0.12	—	15	−0.07	—	14
1974–1991	0.35	—	14	0.42	94	16
1976–1991	0.58	98	14	0.60	99	17
Zebiak and Cane coupled model						
full 100-year record	0.52	99	18	0.56	99	18
"Quiescent ENSO regime" years 1–50	0.45	99	14	0.33	99	16
"Active ENSO regime" years 50–100	0.67	99	18	0.71	99	18
Battisti version of the ZC coupled model	0.92	99	14	0.91	99	15

Unauthenticated | Downloaded 12/05/23 06:20 PM UTC

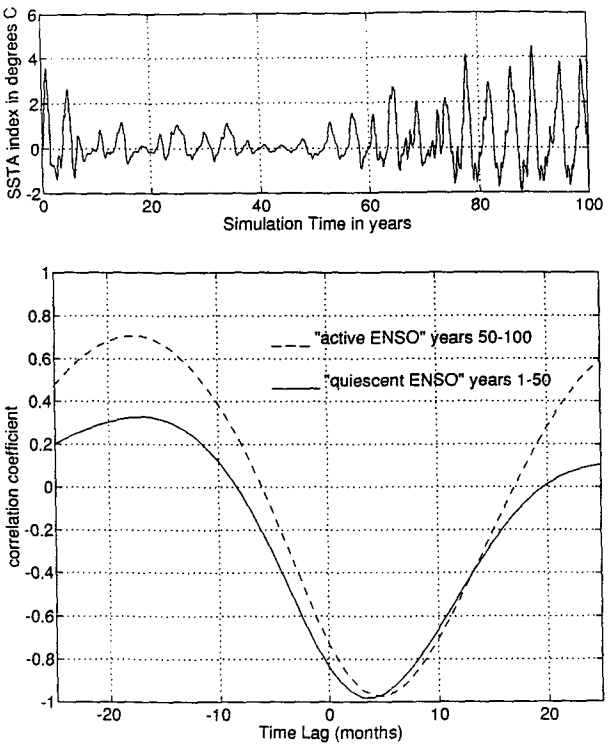

FIG. 3. (a) Time series of NINO3 SST anomalies from a 100-year integration of the standard Zebiak and Cane coupled model. (b) Lag correlations between η_w and the zonal wind stress for the active (solid line) and quiescent (dashed line) ENSO regimes of the Zebiak and Cane coupled model (refer to text for explanation of regimes). A 1-year low-pass filter is applied to the time series before performing correlation analysis.

at a confidence level greater than 99%). Similar though less drastic changes are evident in the η_w leading τ^c correlations (see Table 1). Not surprisingly, when the ENSO cycles are frequent the correlations look like those from the model constructed by Battisti (see Fig. 1b). In years 1–50 when the cycles are weak or nonexistent, the correlations are much less like delayed oscillator theory predicts. We stress that in both the Battisti version of the ZC model and in the active regime of the ZC model, the ENSO cycles are quasi periodic. In this case, the analogous physics responsible for the shutdown of the warm events and the subsequent passage to a cold event are also responsible for the shutdown of the cold event and the subsequent passage into a warm event.

Turning our attention back to the hindcast model output and the historical SST anomaly record (Fig. 2), we ask if there is evidence for ENSO regimes in the 32 years of simulated ocean and observed wind and SST data. From the correlations displayed in Fig. 4 and Table 1 we argue that this is indeed the case. When η_w leads τ^b the peak correlation improves from $r = -0.07$ for 1964–1976 to $r = +0.60$ for 1976 through 1991 (the latter correlation is significant with 99% confidence). Similar though less dramatic differences in the peak correlations between η_w and τ^c are also found in these different periods. Table 1 summarizes the lag correlations discussed in this work.

4. Discussion

When WS (1991) analyzed the output from their ocean model hindcast they found that for nearly every warm or cold ENSO episode the key elements in the delayed oscillator theory were apparent: a westerly (easterly) wind forcing in the central Pacific excited downwelling (upwelling) Kelvin modes to the east, and that same wind forcing raised (depressed) the thermocline to the west in the guise of westward propagating Rossby modes. The Rossby modes were reflected at the western boundary in the form of upwelling (downwelling) Kelvin modes a few months after the initial wind forcing was observed. Finally, these reflected Kelvin modes traveled eastward to the original forcing region where, after typically 1 year of competition with the still westerly (easterly) wind-forced downwelling (upwelling) Kelvin modes to the east, they terminated the local instability (the growing warm event) in the central and eastern Pacific.

With the same ocean model and the same wind forcing used by WS we found that the lag correlations designed to test the delayed oscillator mechanism were very unimpressive. Can these delayed oscillator correlations (and those of LC) be reconciled with the results presented by WS? We present three simple scenarios that alleviate the apparent inconsistencies between the analysis of WS and the delayed oscillator lag correlations presented here (and in LC). The lag correlations between η_w and an index of the zonal wind for the three cases discussed in this section are plotted in Fig. 5d.

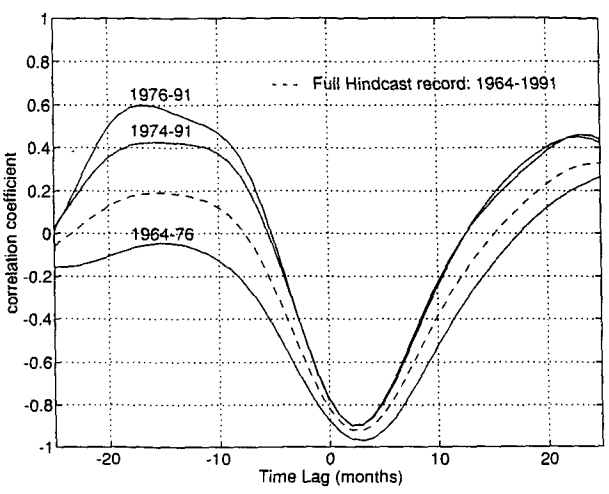

FIG. 4. Lag correlations between η_w and τ^b for selected periods of the hindcast model output. The lag correlations between the "observed" η_w and τ^b from Fig. 1b are also presented (dashed line).

Unauthenticated | Downloaded 12/05/23 06:20 PM UTC

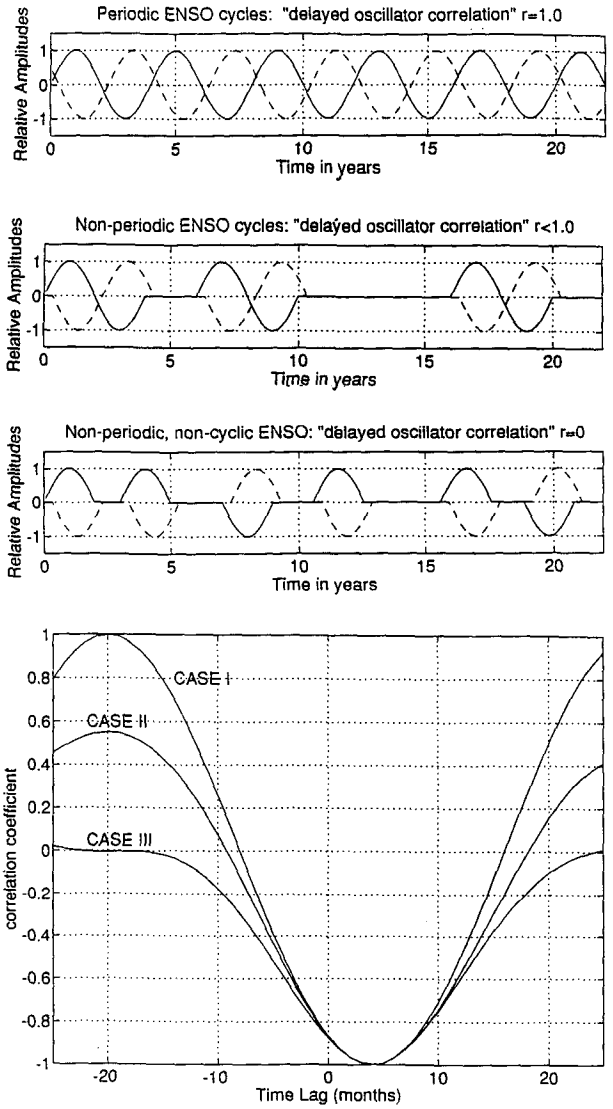

FIG. 5. Synthetic time series of η_w (dashed) and zonal wind index (solid) for: (a) case I, a perfectly periodic, cyclic ENSO system; (b) case II, a system with nonperiodic ENSO cycles; (c) case III, a system with nonperiodic, noncyclic ENSO warm and cold events; and (d) lag correlations between and the zonal wind index for the systems described in cases I, II, and III.

a. Case I: Periodic ENSO cycles

The strong lag correlations found in coupled models that produce perfectly periodic ENSO variability are the result of *a continuous succession of alternating warm and cold events.* Figure 5a shows the characteristic time series for the zonal wind index τ^i (either τ^c or τ^b) and η_w in such a system. For every westerly (warm) event, there is a negative Kelvin mode signature on the western boundary that lags the wind forcing by a few months (a negative correlation, $r = -1$, Fig. 5d). In each episode the retarded forcing associated with the reflected Kelvin mode erodes the local instability and eventually throws the system into a new event of the opposite sign. For every peak in the Kelvin mode time series, there is an extreme value in the zonal wind index of the same sign about a year and a half later (a positive correlation, $r = +1$, Fig. 5d). The sequence of events described in this case is exactly that described by harmonic, delayed oscillator theory. The reflected Kelvin mode is serving two purposes in this system: first as a termination mechanism for the mature ENSO anomalies in the central and eastern Pacific, and then as a trigger for the next event of the opposite sign.

It is well established that the historical ENSO record is not characterized by perfectly periodic alternating warm/cold phases like those depicted in Fig. 5a and evident in the coupled models from which the delayed oscillator theory was spawned.

b. Case II: Nonperiodic ENSO cycles

The time series shown in Fig. 5b depicts a system that has irregularly occurring cycles of warm-to-cold episodes, as in the composite ENSO of Rasmusson and Carpenter (1982). In this case we assume (for the sake of argument) that the warm SST anomaly in the eastern Pacific is initiated by some random perturbation. The atmosphere in the central Pacific displays westerly wind anomalies like those generally observed during the warm phases of ENSO. The SST and wind anomalies grow and decay simultaneously. The western boundary Kelvin mode response again lags the wind forcing by a few months. The delayed forcing carried by the reflected Kelvin modes eventually erase the warm anomalies and then trigger the growth of cold anomalies in the eastern and central Pacific. Unlike the continuous cycles of case I, this system experiences a break in ENSO activity after the cold event. In this example the reflected Kelvin mode that brings the cold event to its end does not initiate another warm event. Note that there is no sign of a Kelvin mode *triggering* the initial instability in the original warm event either. From Fig. 5b it is obvious that there is no connection between the growing westerly wind anomalies (i.e., the growing warm event) and Kelvin mode activity a year and a half in advance, and no sign of positive westerly wind anomalies following the positive Kelvin mode amplitudes from the cold event a year and a half later.

Breaks in ENSO activity are often observed. One example is the relatively quiescent period from late 1974 through the beginning of 1982 (Fig. 2). "Inactive" spells in the coupled ENSO system insure a severe degradation in the delayed oscillator lag correlations where η_w leads the zonal wind index. Nonetheless, the physics of each individual episode depicted in Fig. 5b remains the same: every growing instability generates a delayed, opposed forcing in the form of the reflected Kelvin modes that terminates the ENSO event. Note that the lag correlation associated with this shutdown signal (the zonal wind *leading* η_w by $\sim$3 months) remains intact

Unauthenticated | Downloaded 12/05/23 06:20 PM UTC

in such regimes ($r = -1$, Fig. 5d). If one adopts the viewpoint that the initial perturbation that sets off the instability growth is not an important part of the ENSO evolution, then each event evolves in the exact same way.

c. *Case III: Nonperiodic, noncyclic ENSO events*

In Fig. 5c we show an even more extreme but realistic possibility: the warm anomaly is initiated by something other than a reflected Kelvin mode issued by the preceding cold event, and this time the warm event is not immediately followed by a cold event. No correlation between η_w and the zonal wind indices will exist at lead times on the order of 1 to 1 1/2 years. The reflected Kelvin modes are again responsible for shutting down the growing instability in the central and eastern equatorial Pacific. The τ^i leading η_w correlation remains perfect ($r = -1$) and the evolution of each event remains the same as that described by delayed oscillator theory. The only departure from the delayed oscillator scenario is the lack of a new instability being triggered by the termination signal. We offer the 1982–83 warm ENSO episode as an example of this type of event (Fig. 2).

The lag correlations for the artificial time series associated with each of the three scenarios discussed in this section are plotted in Fig. 5d. In each of the three cases the correlation for τ^i leading η_w by $\sim$3 months agrees perfectly with linear equatorial adjustment theory for a two-level ocean model. On the other hand, the delayed oscillator correlation (for η_w leading τ^i) varies drastically between the three cases. The lag correlations for the three synthetic time series pairs of τ^i and η_w (Fig. 5d) reproduce the major characteristics of the hindcast lag correlations (Fig. 4). Li and Clarke's lag correlations between their reconstructed η_w and the observed zonal wind indices are similar in character to the lag correlations derived from the case II (nonperiodic ENSO cycles) time series.

It is clear from the above discussion that lag correlations between western boundary Kelvin mode amplitudes and equatorial zonal wind indices are not capable of testing the role of reflected Kelvin modes in the ENSO event evolution. What these lag correlations do reveal is the regularity of ENSO cycles (when η_w leads τ^i by 1 to 1 1/2 years) and the existence of reflected Kelvin mode signals on the western boundary (when τ^i leads η_w by a few months). It is important to note that the strong negative correlations for τ^i leading η_w, while robust and apparent in both our hindcast and LC's sea-level data, are consistent with but do not verify the hypothesized role of reflected Kelvin modes as the termination mechanism for ENSO anomalies. A detailed analysis of the thermodynamic and dynamic processes taking place in the central and eastern equatorial Pacific is needed to truly understand the reversal of the coupled ENSO instability.

In the following section we present one test of the potential for reflected Kelvin modes to play the role of the ENSO anomaly termination mechanism.

5. Is the amplitude of the "observed" reflected Kelvin mode sufficient to shut down an ENSO event?

In sections 2 and 3 we demonstrated that the delayed oscillator physics can be acting to shut down ENSO and still yield a weak (near zero) correlation between the western Pacific Kelvin wave amplitude and the zonal wind stress anomaly across the Pacific. We now directly compare the "observed" western Pacific Kelvin wave amplitude from LC with that from the hindcast using the reduced gravity model (Fig. 2b). Since η_w is not directly available from the tide gauge data, Clarke (1992) used the existing tide gauge data off NW Australia and theory for the transmission of equatorial waves through islands to derive the "observed" Kelvin wave amplitude in the far western Pacific. As a result, the signals that can be examined are limited to the interannual and longer time scales. Thus LC applied two passes of a 13-month running mean filter on the observed Kelvin amplitude. We have applied the same filter on the hindcast Kelvin amplitude; both time series are displayed in Fig. 6. Plotted in Fig. 6 are the anomalies about the time mean, where the time mean is calculated for the same time interval for the observations and hindcast η_w, July 1963–May 1985.

The hindcast Kelvin wave amplitude in the western Pacific is in remarkable agreement with that observed. The correlation between the two time series is 0.83. The variance in the observed η_w is about two-thirds of that from the model hindcast: using a linear regression, we find that the observed amplitude is 73% of the hindcast amplitude.

The discrepancy between the amplitude of the observed and hindcast η_w is expected. In the model the incident Rossby signals are reflected off a rigid, perfectly north–south wall. Clarke (1991) and du Penhoat and Cane (1991) have presented theoretical analyses that indicate the realistic geometry of the western Pacific ocean boundary will act to reduce the efficiency of the reflection process (for signals on the interannual time

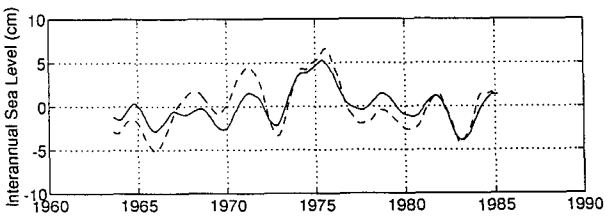

FIG. 6. Time series of the amplitude of the sea level perturbation in the far western Pacific, η_w, observed (solid curve, from LC) and hindcast (dashed curve). Two passes of a 13-month running mean filter have been applied to the data.

Unauthenticated | Downloaded 12/05/23 06:20 PM UTC

scale). Since the amplitude of the Kelvin mode issued from the western boundary during ENSO is largely due to the first meridional Rossby mode (Battisti 1988; WS), we can estimate [using the results of Clarke (1991)] that by using a more realistic western boundary geometry the hindcast η_w will be reduced by about 17% (there is little effect on the phase). Thus, taking into account the reduction in η_w due to the realistic geometry, the difference between the amplitude of the observed and the hindcast η_w is only about 13% [1–0.73/(1–0.17)]. This result adds to the ample existing evidence that supports the use of rather simple dynamical models for the study of low-frequency tropical ocean variability.

Finally, BH have demonstrated that the amplitude of the Kelvin mode in the far western Pacific—issued from the western boundary due to the incident Rossby waves—must be greater than 55% of that in the pure reflection case (i.e., that obtained in Fig. 2b) if the delayed oscillator physics is to operate to shut down the ENSO events in the ZC model. The results presented in Fig. 6 suggest that the amplitude of the observed η_w at the western boundary is 73% of the hindcast signal (the latter allows a "perfect" reflection). Thus, the amplitude of the observed Kelvin signal is well in excess of the minimum signal that is required to shut down the model ENSO events *via* the delayed oscillator physics.

6. Summary

We set out to investigate the apparent discrepancies between the correlations predicted by delayed oscillator theory and those calculated from observations by LC. First, from the results of a hindcast of ocean variability we find that the correlations between modeled western boundary Kelvin mode amplitudes and equatorial zonal wind indices are consistent with the correlations presented by LC. We have also shown that the latter half of the hindcast record displays much stronger "delayed oscillator" lag correlations than the early half. Similar behavior is apparent in the output of a standard integration of the ZC coupled ocean–atmosphere model that displays prolonged periods of first quiescent and then active ENSO variability.

We have shown that lag correlations between η_w and zonal wind indices are sensitive to the frequency and character of the interannual variability in the system being studied. Historical SST and zonal wind anomalies (Fig. 2) suggest that a mix of the three behaviors depicted in idealized cases I, II, and III of section 4 constitute the observed ENSO system: sometimes quasi-periodic, sometimes cyclic, and sometimes episodic.

The simple scenarios presented in the discussion question the reliability of η_w–zonal wind correlations as an accurate test of the role of reflected Kelvin modes as a termination mechanism for ENSO anomalies: Low "delayed oscillator" lag correlations can result from the western boundary reflections acting mainly as a termination mechanism for the warm events. The existence of reflected Kelvin modes in the western Pacific is strongly supported by the time series presented by LC, and from our hindcast calculation (see also WS and Kessler 1991). A regression analysis between the observed zonal wind and tide gauge reconstructed η_w shows that reflected Kelvin mode amplitudes are sufficient to reverse the local instabilities in the central and eastern equatorial Pacific that are associated with mature ENSO anomalies.

Records of observed and hindcast tropical climate variability (e.g., the NINO3 SST anomalies in Fig. 2, the FSU zonal stress indices, and hindcast η_w in Fig. 6) do not support the view that reflected Kelvin modes from the demise of a cold event act as a reliable *trigger* for the next warm event. Lag correlations between η_w and indices of the zonal wind stress do, however, test the *regularity* of a coupled ENSO system governed by delayed oscillator physics. Delayed oscillator theory, in its most literal sense, describes a perfectly periodic system that supports a never-ending succession of alternating warm and cold cycles. As applied to the coupled intermediate models and to this study, this theory describes the termination of growing instabilities in the central and eastern equatorial Pacific. The lack of regularity that is a key part of the observed tropical Pacific climate system is not contained in, nor explained by, delayed oscillator theory. However, the episodic nature and the evolution of wind and SST anomalies in each (warm or cold) event remains consistent with the major features of the delayed oscillator scenario. The only missing ingredient is the initial perturbation, trigger if you will, for the instability in the central and eastern Pacific to act on.

Acknowledgments. We thank M. Cane and S. Zebiak for providing their model code. This study was supported by grants from NASA's Global Change Fellowship Program, the NOAA TOGA Office, and from the NOAA Equatorial Pacific Ocean Climate Studies (EPOCS) program of the University of Washington's Experimental Climate Forecast Center (ECFC).

REFERENCES

Battisti, D. S., 1988: Dynamics and thermodynamics of a warming event in a coupled tropical atmosphere–ocean model. *J. Atmos. Sci.*, **45**, 2889–2919.

——, and A. C. Hirst, 1989: Interannual variability in a tropical atmosphere–ocean model: Influence of the basic state, ocean geometry and nonlinearity. *J. Atmos. Sci.*, **46**, 1687–1712.

Busalacchi, A. J., and J. J. O'Brien, 1981: Interannual variability of the equatorial Pacific in the 1960s. *J. Geophys. Res.*, **86**, 10 901–10 907.

——, K. Takeuchi, and J. J. O'Brien, 1983: Interannual variability of the equatorial Pacific: Revisited. *J. Geophys. Res.*, **88**, 7551–7562.

Cane, M. A., and E. S. Sarachik, 1979: Forced baroclinic ocean motions, III: The linear equatorial basin case. *J. Mar. Res.*, **37**, 355–398.

Unauthenticated | Downloaded 12/05/23 06:20 PM UTC

Clarke, A. J., 1991: On the reflection and transmission of low-frequency energy at the irregular western Pacific Ocean boundary. *J. Geophys. Res.*, **96**(Suppl.), 3289–3305.

——, 1992: Low-frequency reflection from a non-meridional eastern ocean boundary and the use of coastal sea level to monitor eastern Pacific equatorial Kelvin waves. *J. Phys. Oceanogr.*, **22**, 163–183.

du Penhoat, Y., and M. A. Cane, 1991: Effect of low-latitude western boundary gaps on the reflection of equatorial motions. *J. Geophys. Res.*, **96**, 3307–3322.

Gill, A. E., 1981: An estimation of sea level and surface current anomalies during the 1972 El Niño and consequent thermal effect. *J. Phys. Oceanogr.*, **13**, 586–606.

Kessler, W. S., 1991: Can reflected extra-equatorial Rossby waves drive ENSO. *J. Phys. Oceanogr.*, **21**, 444–452.

Kubota, M., and J. J. O'Brien, 1988: Variability of the upper tropical Pacific ocean model. *J. Geophys. Res.*, **93**, 13 930–13 940.

Legler, D. M., and J. J. O'Brien, 1988: Tropical Pacific wind stress analysis for TOGA. *IOC Time Series of Ocean Measurements*, IOC Technical Series 33, Vol. 4, UNESCO.

Li, B., and A. J. Clarke, 1984: An examination of some ENSO mechanisms using interannual sea level at the eastern and western equatorial boundaries and the zonally averaged equatorial wind. *J. Phys. Oceanogr.*, **24**, 681–690.

Rasmusson, E. M., and T. H. Carpenter, 1982: Variations in tropical sea surface temperatures and surface wind fields associated with the Southern Oscillation and El Niño. *Mon. Wea. Rev.*, **110**, 354–384.

Schopf, P. S., 1987: Coupled dynamics of the tropical ocean atmosphere system. *TOGA Workshop on the Dynamics of the Equatorial Oceans*, Honolulu, Hawaii, TOGA, Katz and Witte, 279–287.

——, and M. J. Suarez, 1988: Vacillations in a coupled ocean–atmosphere model. *J. Atmos. Sci.*, **45**, 549–566.

Suarez, M. J., and P. S. Schopf, 1989: A delayed action oscillator for ENSO. *J. Atmos. Sci.*, **45**, 3283–3287.

Wakata, Y., and E. S. Sarachik, 1991: On the role of equatorial ocean modes in the ENSO cycle. *J. Phys. Oceanogr.*, **21**, 434–443.

White, W. B., B. Meyers, J. R. Donguy, and S. Pazan, 1985: Short-term climatic variability in the thermal structure of the Pacific Ocean during 1979–82. *J. Phys. Oceanogr.*, **15**, 917–935.

——, Y. He, and S. E. Pazan, 1989: Off-equatorial westward propagating waves in the tropical Pacific during the 1982–83 and 1986–87 ENSO events. *J. Phys. Oceanogr.*, **19**, 1397–1406.

Zebiak, S. E., 1989: Oceanic heat content variability and El Niño cycles. *J. Phys. Oceanogr.*, **19**, 475–486.

——, and M. A. Cane, 1987: A model El Niño–Southern Oscillation. *Mon. Wea. Rev.*, **115**, 2262–2278.

Unauthenticated | Downloaded 12/05/23 06:20 PM UTC